

$\approx 2 \times 10^{-8} \eta$ for the 100-keV electrons typical of β decay. This last result is directly relevant to the question of the origin of optical activity in living organisms since, if β -decay electrons are the cause of optical activity (the Vester-Ulbricht hypothesis),^{17,18} the specific mechanism involved is most likely a slight asymmetric ionization or excitation of the *D* isomer with respect to the *L* isomer, followed by chemical and biological amplification. The small value of the difference indicated above is discussed by Gidley *et al.*¹⁴ in the context of recent experiments to detect such effects.

In summary we have made a quantitative calculation of a CES process and we are now extending this initial work to other CES phenomena. Features of inelastic electron and positron interactions with chiral targets can also be investigated by the techniques described in this article.

We thank G. W. Ford, D. W. Gidley, and P. W. Zitzewitz for helpful discussions. This work was supported by the National Aeronautics and Space Administration under Grant No. NSG7452 and by the National Science Foundation under Grant No. PHY81-07573.

¹L. D. Barron and A. D. Buckingham, *Annu. Rev.*

Phys. Chem. **26**, 381 (1975). For more recent work, see L. A. Nafie and T. B. Friedman, *J. Chem. Phys.* **75**, 4847 (1981), and references therein.

²P. K. Kabir, G. Karl, and E. Obryk, *Phys. Rev. D* **10**, 1471 (1974). For more recent work, see J. N. Cox and F. S. Richardson, *J. Chem. Phys.* **73**, 1591 (1979), and references therein.

³R. A. Harris and L. Stodolsky, *J. Chem. Phys.* **70**, 2789 (1979).

⁴M. Forte *et al.*, *Phys. Rev. Lett.* **45**, 2088 (1980).

⁵M. J. M. Beerlage, P. S. Farago, and M. J. Van der Wiel, *J. Phys. B* **14**, 3245 (1981).

⁶P. S. Farago, *J. Phys. B* **13**, L567 (1980).

⁷P. S. Farago, *J. Phys. B* **14**, L743 (1981).

⁸V. A. Kizel, *Usp. Fiz. Nauk* **23**, 209 (1980) [*Sov. Phys. Usp.* **23**, 277 (1980)].

⁹L. Keszthelyi, *Origins Life* **11**, 9 (1981).

¹⁰R. A. Hegstrom, to be published.

¹¹A. S. Garay and P. Hrasko, *J. Mol. Evol.* **6**, 77 (1975).

¹²J. R. Taylor, *Scattering Theory* (Wiley, New York, 1972).

¹³R. A. Hegstrom, D. W. Rein, and P. G. H. Sandars, *J. Chem. Phys.* **73**, 2329 (1980).

¹⁴D. W. Gidley, A. Rich, J. C. Van House, and P. W. Zitzewitz, to be published.

¹⁵D. W. Gidley, A. Rich, J. C. Van House, and P. W. Zitzewitz, *Origin of Life* (Reidel, Boston, 1981), p. 379, and *Origins Life* **11**, 31 (1981).

¹⁶A. Rich, *Rev. Mod. Phys.* **53**, 127 (1981).

¹⁷H. Krauch and F. Vester, *Naturwissenschaften* **44**, 49 (1957).

¹⁸T. L. V. Ulbricht, *Q. Rev.* **13**, 48 (1959).

Experimental Detection of HOC⁺ by Microwave Spectroscopy

Christopher S. Gudeman and R. Claude Woods

Department of Chemistry, University of Wisconsin, Madison, Wisconsin 53706

(Received 29 March 1982)

Microwave spectroscopy has been employed to make the first definite experimental observation of the ionic metastable isomer HOC⁺. Its $J = 0 \rightarrow 1$ transition and those of its ¹⁸O and ¹³C isotopic variants have been detected in laboratory dc glow discharges. Extensive chemical, spectroscopic, and theoretical evidence permits conclusive identification of these spectra. Comparison of the substitution bond lengths [$r_s(\text{CO}) = 1.1595 \text{ \AA}$ and $r_s(\text{OH}) = 0.9342 \text{ \AA}$] to *ab initio* structures strongly supports a large-amplitude (low-frequency) bending vibration.

PACS numbers: 33.20.Bx, 35.20.Dp, 52.80.Hc, 98.40.Ct

While HCN, HNC, HN₂⁺, and HCO⁺ have been extensively studied by molecular radioastronomy^{1,2} and laboratory high-resolution spectroscopy,³⁻⁵ the obvious missing member of this iso-electronic series of molecules, HOC⁺, has never been detected with certainty in either space or laboratory experiments. The first four molecules

have been shown to be widely distributed in the interstellar medium and extremely important as participants in its chemistry and useful as radio-astronomical probes of its physical conditions.¹ Furthermore, their molecular structures and other properties as determined from high-resolution spectroscopy have provided very satisfying tests

of the results of numerous high-level *ab initio* theoretical calculations.²⁻⁵ We report here a definitive spectroscopic observation of HOC^+ , a metastable ionic isomer which promises to be of similar widespread interest. Ordinary mass spectrometry fails to distinguish HOC^+ from its ever-present stable isomer HCO^+ , but Berkowitz⁶ has characterized his more sophisticated photoionization mass spectrometry experiments on deuterated methanol (CD_3OH) as providing "mild support" for the existence of HOC^+ , while pointing out the possibility of other interpretations of his data. The initial *ab initio* theoretical characterization of HOC^+ came from self-consistent-field (SCF) calculations by Jansen and Ros,⁷ who predicted the structures, isomerization energy, and isomerization barrier for HCO^+ and HOC^+ and suggested a much lower bending force constant for the latter. Several other SCF level computations on HOC^+ have since been published,⁸⁻¹⁰ and these papers provide much discussion and many data on its properties, its relation to similar species, and the nature of its chemical bonding. In 1976 Herbst *et al.*¹¹ published the first configuration interaction (CI) calculations on HOC^+ ; they predicted the $J=0-1$ transition to occur at 88 830 MHz on the basis of their computed structure and discussed the prospects for finding this ion in the interstellar medium. Hennig, Kraemer, and Dierksen¹² have carried out consistent and extensive large-basis-set calculations with very large CI wave functions on HOC^+ and the other four previously mentioned molecules. They have computed equilibrium structures, harmonic and anharmonic force fields, vibrational frequencies, vibration-rotation interaction constants (α 's), and B_0 's (ground-state rotational constants) for all reasonable isotopic forms. Correcting their frequency prediction ν_{SDQ} (singles, doubles, and quadruples CI) for HOC^+ by the average of the ratio $\nu_{\text{expt}}/\nu_{\text{SDQ}}$ for the other four species yields $\nu = 89\,400_{-100}^{+1000}$ MHz where the error range shown indicates the total scatter in the four known cases. A recent high-quality calculation on HOC^+ along with HCO^+ , HCN , and HNC by Nobes and Radom¹³ used a third-order Moller-Plesset treatment of electron correlation. They predict an equilibrium structure and a transition frequency of $89\,000 \pm 800$ MHz for HOC^+ , an energy relative to HCO^+ of 157 kJ/mol, and an isomerization barrier of 150 kJ/mol. No theoretical dipole moment appears to have been reported for HOC^+ , but Haese and Woods¹⁴ have argued that it should be near 4 D, i.e., about the

same as that for HCO^+ .

The present experiments utilized the same basic technique as earlier studies of CO^+ ,¹⁵ HCO^+ ,^{3,16} HN_2^+ ,^{4,17} and HCS^+ ¹⁸ in this laboratory, but a new vacuum system-discharge tube combination with a 10-cm-diam by 3-m-long absorption cell that will be described in a subsequent article¹⁹ was employed. This cell was liquid nitrogen cooled and pumped with a large oil-diffusion pump in all the work reported here. The phase-lock method, modulation scheme, computer control, and data processing procedures were the same as those used for HCS^+ ,¹⁸ and will be described in detail later.¹⁹ With the goal of locating both the HOC^+ transition and the vibrational satellites of HCO^+ , we carried out a careful search (requiring several weeks) over the entire region from 88 200 to 89 800 MHz with a mixture of 15-20 mTorr argon and 0.5 mTorr each of hydrogen and carbon monoxide. These conditions, which routinely produce a signal-to-noise ratio of 500/1 for the $J=0-1$ transition of HCO^+ , were suggested to us by a long series of experiments, whose results will be published separately, on the pressure broadening²⁰ and Doppler shifts¹⁹ of the HCO^+ transition in a variety of carrier gases. Other than the ground-state lines of HCO^+ and HCN , one formaldehyde line, and several previously identified²¹ lines of $a^3\Pi$ CO, we found only two narrow lines that were clearly due to neutrals on the basis of their linewidth, and four broad lines that appeared to be ionic in origin on the basis of theirs. [The earlier pressure-broadening experiments²⁰ had shown the HCO^+ (or HN_2^+) linewidth to be about 3-4 times greater than any neutrals', e.g., HCN 's, in the argon carrier gas.] Three of those broad lines were eventually assigned to the (100), (02⁰), and (001) vibrational satellites of HCO^+ and will be reported in a separate article on the equilibrium structures of HCO^+ ,²² while the fourth, found near 89 487 MHz, is the subject of the present paper. The optimum partial pressures of CO and H_2 for producing it were found to be 0.5 mTorr each, where its intensity was still 40-50 times weaker than that of the HCO^+ line, and it could not be detected at all except in a large excess of argon. Mixtures of $\text{Ar-CH}_4\text{-O}_2$ or $\text{Ar-CH}_4\text{-CO}$ (in the same proportions) worked equally well and slightly better, respectively. A spectrum under optimum conditions is shown in Fig. 1.

Despite considerable effort we were not able to measure a statistically significant Doppler shift on the 89 487-MHz line when the discharge polar-

ity was reversed, but this is not surprising for this relatively weak line, since the shift we obtained for HCO^+ under these conditions was only 8 kHz. We did obtain a pressure-broadening parameter, $\Delta\nu/P = 15 \pm 4$ MHz/Torr, by measuring the linewidth over the pressure range 8–40 mTorr, and this is the same within experimental error as that for HCO^+ in argon. The addition of very small amounts of N_2 actually decreased the intensity of the line, showing that the species responsible does not contain nitrogen. The HO^{13}C^+ line was predicted to be at $(89\,487\text{ MHz})(\nu_{13,\text{SDQ}}/\nu_{12,\text{SDQ}}) = 85\,760$ MHz from the ν_{SDQ} 's of Hennig, Kraemer, and Dierksen¹² and quickly found at 85 753 MHz using 90% enriched ^{13}CO . This line was also broad and was formed equally well in $\text{Ar-}^{13}\text{CO-H}_2$ or $\text{Ar-}^{13}\text{CH}_4\text{-O}_2$, with the same optimum partial pressures, clearly indicating that it came from the same molecule. An extensive series of isotopic mixing experiments showed that both the 89 487-MHz line and the 85 753-MHz line came from molecules with exactly one hydrogen atom, one carbon atom, and one oxygen atom. For example, when 0.25 mTorr $\text{CO-}^{13}\text{CO}$ was substituted for 0.5 mTorr CO , the intensity of the 89 487-MHz line fell by just a factor of 2, indicating exactly one carbon atom. Neither line showed any nearby related lines, incompletely resolved hyperfine structure, or sensitivity to applied magnetic field. Location of the spectrum of the ^{18}O species proved to be rather difficult. A repeated search of a 300-MHz region (using 99% C^{18}O or $^{18}\text{O}_2$) yielded only a sin-

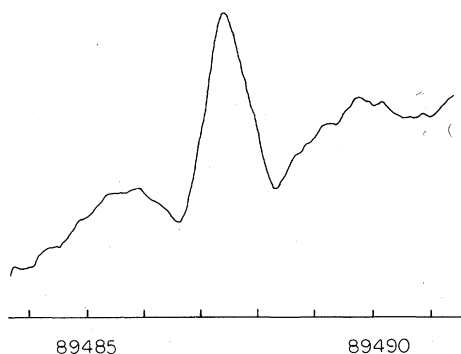


FIG. 1. The $J=0 \rightarrow 1$ transition of HOC^+ observed in a fast-flowing 15-mTorr Ar discharge with 0.5 mTorr each of CO and CH_4 , 200 mA discharge current, and liquid-nitrogen cooling. This spectrum is the average of 1580 scans, each consisting of 1000 points and collected at a rate of 2 msec/point with a 1-msec lock-in time constant. Digital smoothing (51-point interval) and baseline suppression have been applied to this data.

gle line, the previously identified²¹ $\nu=2$, negative-parity, $J=0 \rightarrow 1$ transition of $a^3\Pi \text{C}^{18}\text{O}$ at 86 611.28 MHz. Finally we realized that the H^{18}OC^+ line must be blended with this one and used the Zeeman effect (obtained by applying the 60-Hz, 120-V power line to a pair of Helmholtz coils) to split apart the $a^3\Pi \text{C}^{18}\text{O}$ transition. The ion line was indeed readily observed only 300 kHz away from the original center frequency of the metastable carbon monoxide transition as shown in Fig. 2. The final measured frequencies for HOC^+ , HO^{13}C^+ , and H^{18}OC^+ are 89 487.414(15), 85 752(15), and 86 611.560(70) MHz, respectively. Each of these is an average of the results from least-squares line-shape analyses of a number of individual spectra, and the errors shown should encompass both random and systematic contributions.

From the available experimental data we can calculate the principal-axis coordinates of C and O with Kraitchman's equation²³ and that of H with the center-of-mass condition. The resulting r_s structure is given in row 1 of Table I, and the predicted r_e structures from the three correlat-

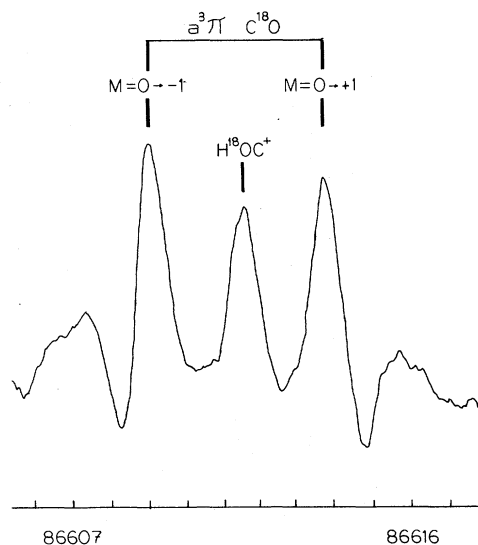


FIG. 2. $J=0 \rightarrow 1$ H^{18}OC^+ and $J=0 \rightarrow 1$, $\nu=2(-)$ $a^3\Pi \text{C}^{18}\text{O}$. Conditions: 0.4 mTorr each of CH_4 and $^{18}\text{O}_2$, 21 mTorr Ar, 200 mA discharge current, fast flow, 51-point smoothing, baseline suppression, 512 scans, 1-msec time constant, 2 msec/point. A 60-Hz magnetic field (~ 8 G rms) was applied in order to split the $a^3\Pi \text{C}^{18}\text{O}$ transition into $\Delta M = \pm 1$ components, thus exposing the H^{18}OC^+ line. The $a^3\Pi \text{C}^{18}\text{O}$ features are distorted and artificially broadened by the time-varying magnetic field; at zero field the CO line is much stronger and narrower than the HOC^+ one.

TABLE I. Theoretical and experimental structures for HOC^+ and related molecules in angstroms.

Structure type	r_{XY}	r_{HX}
HOC ⁺		
r_s (expt) ^a	1.1595	0.9342
r_s (SDQ) ^{a,b}	1.1617	0.9585
r_e (SDQ) ^c	1.1584	0.9910
r_e (CI) ^d	1.159	0.976
r_e (MP3-corr) ^e	1.155	0.988
HNC		
r_s (expt) ^a	1.1717	0.9731
r_s (SDQ) ^{a,b}	1.1748	0.9872
r_e (SDQ) ^c	1.1719	0.9979
HCN		
r_s (expt) ^a	1.1551	1.0603
r_s (SDQ) ^{a,b}	1.1597	1.0628
r_e (SDQ) ^c	1.1583	1.0668

^aThe H principal-axis coordinate was obtained from the center-of-mass condition in all cases.

^bCalculated from B_0 's of Ref. 12 using Kraitchman's equation.

^cRef. 12.

^dRef. 11.

^eRef. 13.

ed electron *ab initio* treatments¹¹⁻¹³ are given in rows 3-5 for comparison. The heavy-atom distance is in excellent agreement with theory, while the OH distance appears far too short. The latter discrepancy is, however, not unexpected, but rather is symptomatic of the low-frequency bending vibration in HOC^+ . Since Hennig, Kraemer, and Dierksen¹² have computed purely theoretical B_0 values, we can use them (for the same three isotopic forms) to obtain a theoretical r_s structure, which is shown in row 2 of Table I. This table also exhibits the corresponding data for HNC and HCN. [The predicted (SDQ) bending frequencies of HOC^+ , HNC, and HCN are 326, 501, and 743 cm^{-1} , respectively.¹²] Clearly for the OH distance in HOC^+ we have $r_s(\text{expt}) \ll r_s(\text{SDQ}) \ll r_e(\text{SDQ})$. For the HX distance of the other two molecules the order is the same, but the effect is much less dramatic in HNC (medium bending frequency) and almost negligible in HCN (fairly high bending frequency). That the experimental r_s 's are even more shortened than the theoretical r_s 's correlates well with the fact that the SDQ bending frequencies are consistently higher than the experimental ones in known cases. Similarly shortened $r_s(\text{OH})$'s have also been

seen in CsOH and RbOH ,²⁴ which have bending frequencies of 306 and 309 cm^{-1} . Thus the microwave frequencies and resultant r_s structure we have obtained for HOC^+ are in essentially perfect harmony with theoretical predictions, confirming the assignment of these spectra beyond any reasonable doubt. The exact shape of the bending potential, which may possibly even exhibit the phenomenon of quasilinearity (a small bump at the linear configuration), will require much additional spectroscopic data. In future work we plan to look for other isotopic forms, vibrational satellites, and higher J transitions. Efforts to observe HOC^+ in the interstellar medium are currently under way.

This work was supported by the Wisconsin Alumni Research Foundation and the National Science Foundation Structural Chemistry Program.

¹W. D. Watson, *Rev. Mod. Phys.* **48**, 513 (1976), and original references therein.

²R. J. Saykally and R. C. Woods, *Annu. Rev. Phys. Chem.* **32**, 403 (1981), and original references therein.

³R. C. Woods, R. J. Saykally, T. G. Anderson, T. A. Dixon, and P. G. Szanto, *J. Chem. Phys.* **75**, 4256 (1981).

⁴P. G. Szanto, T. G. Anderson, R. J. Saykally, N. D. Pillich, T. A. Dixon, and R. C. Woods, *J. Chem. Phys.* **75**, 4261 (1981).

⁵References 3 and 4 give original references to much of the theoretical and spectroscopic work on these molecules up to mid 1981.

⁶J. Berkowitz, *J. Chem. Phys.* **69**, 3044 (1978).

⁷H. B. Jansen and P. Ros, *Chem. Phys. Lett.* **3**, 140 (1969).

⁸S. Forsén and B. Roos, *Chem. Phys. Lett.* **6**, 128 (1970).

⁹P. J. Bruna, S. D. Peyerimhoff, and R. J. Buenker, *Chem. Phys.* **10**, 323 (1975).

¹⁰N. L. Summers and J. Tyrrell, *J. Am. Chem. Soc.* **99**, 3960 (1977), and *Theor. Chim. Acta* **47**, 223 (1978).

¹¹E. Herbst, J. M. Norbeck, P. R. Certain, and W. Klemperer, *Astrophys. J.* **207**, 110 (1976).

¹²P. Hennig, W. P. Kraemer, and G. H. F. Dierksen, unpublished.

¹³R. H. Nobes and L. Radom, *Chem. Phys.* **60**, 1 (1981).

¹⁴N. N. Haese and R. C. Woods, *J. Chem. Phys.* **73**, 4521 (1980).

¹⁵T. A. Dixon and R. C. Woods, *Phys. Rev. Lett.* **34**, 61 (1975).

¹⁶R. C. Woods, T. A. Dixon, R. J. Saykally, and P. G. Szanto, *Phys. Rev. Lett.* **35**, 1269 (1975).

¹⁷R. J. Saykally, T. A. Dixon, T. G. Anderson, P. G. Szanto, and R. C. Woods, *Astrophys. J. Lett.* **205**, L101 (1976).

¹⁸C. S. Gudeman, N. N. Haese, N. D. Piltch, and R. C. Woods, *Astrophys. J. Lett.* **246**, L47 (1981).

¹⁹C. S. Gudeman, N. D. Piltch, and R. C. Woods, to be published.

²⁰C. S. Gudeman, N. D. Piltch, and R. C. Woods, to be published.

²¹R. J. Saykally, T. A. Dixon, T. G. Anderson, P. G. Szanto, and R. C. Woods, to be published.

²²C. S. Gudeman and R. C. Woods, to be published.

²³J. Kraitchman, *Am. J. Phys.* **21**, 17 (1953).

²⁴D. R. Lide and C. Matsumura, *J. Chem. Phys.* **50**, 3080 (1969).

Simultaneous Observation of Caviton Formation, Spiky Turbulence, and Electromagnetic Radiation

P. Y. Cheung, A. Y. Wong, C. B. Darrow, and S. J. Qian

Department of Physics, University of California, Los Angeles, California 90024

(Received 21 October 1981)

Formation of density cavities, spiky turbulence, and electromagnetic radiation at the plasma frequency (ω_p) and its harmonics are observed simultaneously in the presence of a cold-electron beam. The electrostatic and electromagnetic frequency spectra evolve with the development of cavities.

PACS numbers: 52.25.Ps, 52.35.Ra

We wish to present experimental observations of the coexistence of large density cavities, spiky turbulence, and the generation of electromagnetic radiation at the fundamental and harmonics of the plasma frequency. Our experiments show that a nearly monochromatic Langmuir wave at a frequency near the ambient plasma frequency (ω_p) is excited by a cold-electron beam without external modulation. The unstable wave is so intense that a density cavity as much as $\delta n/n_0 \approx 50\%$ (δn is the change in density and n_0 is the plasma density) is created in a uniform, unmagnetized plasma. New unstable electrostatic waves are subsequently excited by the beam inside the cavity at the lower plasma frequency corresponding to the depressed density of the cavity. These waves, which are evanescent outside the cavity, are trapped and can be driven to spatially localized structures of wave intensity E_{es}^2 . Spiky turbulence here is defined as a significant (more than an order of magnitude) spatial localization of the wave intensity. The most intense peaks observed have a spatial extent of the order of 12 Debye lengths, which is approximately one-sixteenth the wavelength of the initial unstable waves.

The results reported in this paper differ from recently published work¹⁻³ in that very large density cavities are measured; a shift in the unstable frequency is observed as the local density is modified and the electromagnetic radiation at $2\bar{\omega}_p$ is comparable in intensity to that at $\bar{\omega}_p$ ($\bar{\omega}_p$

is the perturbed plasma frequency of the density cavity). It is distinctly different from previous work on Langmuir-wave turbulence^{4,5} because a fast electron beam is used with $v_b/v_e \geq 30$ and no external modulation is applied in the present experiments; v_b and v_e are the beam velocity and electron thermal velocity, respectively. The most unstable wave grows from noise and has a narrow frequency width of $\delta\omega/\omega_p \lesssim 3\%$.

The experiments are performed in a large (1.8 m long and 1.8 m wide) vacuum chamber. The background plasma is uniform and unmagnetized, and is produced independently of the electron beam by pulsed filament discharge in argon gas. Each experiment is performed in an afterglow plasma with typical plasma parameters of $T_e = 1.5$ eV and $n = 2.3 \times 10^9$ cm⁻³ where T_e is the electron temperature. The electron beam is also pulsed, has a typical pulse duration of $\tau_b = 13$ μ s, and is injected into the background plasma approximately 700 μ s after the background plasma is shut off. The beam has a diameter of approximately 4 cm and is produced by a hot-cathode source. It has a beam voltage of $V_b = 800$ V, a beam spread of $\Delta v/v_b \approx 2\%$, where Δv is the beam velocity spread, and beam densities of $n_b/n_0 = (0.2-4)\%$. Electrostatic potential and electric field fluctuations are measured by high-frequency probes that have either a single wire tip (3 mm long, 0.5 mm diam) or two wire tips closely spaced together. Beam characteristics are measured by double-sided Langmuir probes and a mul-